02

Spectroscopy of f^{13}- lanthanides in fluoride crystals

© E.A. Radzhabov[1], R.Yu. Shendrik[1], V. Pankratov[2]

[1] Vinogradov Institute of Geochemistry, Siberian Branch, Russian Academy of SciencesIrkutsk, 664033 Irkutsk, Russia
[2] The Institute of Solid State Physics, University of Latvia, LV1063 Riga, Latvia
e-mail: eradzh@igc.irk.ru

Received October 17, 2022
Revised February 15, 2023
Accepted February 19, 2023

The absorption and luminescence spectra of $4f-4f$- transitions of Yb^{3+} ions in crystals of CaF_2, SrF_2 and BaF_2 fluorides have been studied. The crystal splitting of the $^2F_{7/2}$, $^2F_{5/2}$ levels in Tm^{2+}, Yb^{3+} by the cubic field decreases linearly with increasing lattice constant. Both lines intersect at the energy of $^2F_{7/2}-^2F_{5/2}$ transitions in unperturbed Tm^{2+}, Yb^{3+} ions. The positions of the f^{13}- levels of Tm^{2+} or Yb^{3+} in fluoride crystals are well described by ab-initio relativistic calculations

Keywords: absorption spectra, emission spectra, f^{13}- levels, alkaline-earth fluorides.

DOI: 10.61011/EOS.2023.04.56352.54-22

Introduction

The structure of the atomic levels of lanthanides (and actinides) with the configuration f^{13} (and f^1) is the simplest among the lanthanides. Owing to the spin-orbit interaction, 14 degenerate states are split into two groups: ground $^2F_{7/2}$ and excited $^2F_{5/2}$. In the octahedral environment of Oh lanthanide ions $4f^{13}$-, the $^2F_{7/2}$ state splits into three (D_6, D_7, D_8 — according to Bethe notation [1,2]), and the excited state $^2F_{5/2}$ splits into two (D_7, D_8). The dependence of the crystal splitting on the lattice constant is studied in detail in this paper by experimental and computational methods.

Halide crystals doped with Tm^{2+} are actively studied in connection with their potential use as solar radiation concentrators [3]. Tm^{2+} radiation in the infrared area can be converted into electrical energy [4].

The aim of our studies was to study the structure of the f^{13} levels of cubic Tm^{2+} and Yb^{3+} centers in fluoride crystals (CaF_2, SrF_2, BaF_2).

Experimental methodology

MeF_2 (Me — Ca, Sr, Ba) crystals were grown by the Bridgman method in a six-barreled graphite crucible in vacuum [5]. A few percent of CdF_2 was added to the raw material to remove oxygen impurities. Crystals of alkaline earth fluorides activated by Tm or Yb were grown (the introduced concentration was $0.01-10$ mol.%). In a number of crystals, a certain fraction of Yb^{3+} ions (approximately 10%) during growth was transformed into a divalent form.

Absorption spectra in the $190-3000$ nm area were measured on an Perkin-Elmer Lambda-950 spectrophotometer. The luminescence spectra in the area of $200-890$ nm were measured using an MDR2 monochromator and a Hamamatsu H6780- photomodule. The luminescence spectra in the long-wavelength region were measured by a cooled PMT83 photomultiplier, a photodetector with a cooled Ge- photodiode FPU- FDG LOMO-PHOTONIKA (up to 1600 nm) and a cooled photoresistor PbS-FSV19AA (up to 2500 n m).

The emission spectra of $f-f$ Tm^{2+} and Yb^{3+} at low temperatures consist of two narrow lines and a vibronic wing towards the long wavelength. The MeF_2-Yb luminescence was excited by laser radiation at a wavelength of 940 nm, as well as by vacuum ultraviolet in the $6-9$ eV area at the FINESTLUMI [6] photoluminescent station of the MAXIV synchrotron facility (Lund, Sweden).

Scheme of calculation

The f- schemes of the levels of Tm^{2+} and Yb^{3+} in fluoride crystals were calculated using the ORCA 5.0.3 [7] software package. Relativistic effects were taken into account by the ZORA [8] method. The basis functions ZORA-def2-TZVP for ligands and SARC2-ZORA-QZVP for the f^{13} ion were used for the calculation. TmF_8 (or TmF_8Me_{12}) cluster was surrounded by point charges (approximately1000 charges) to simulate a crystal field.

In accordance with the recommendations [8], the calculation of f-levels was carried out in three steps. At the first step, the initial orbitals of the cluster were calculated. At the second step, the initial orbitals were used and seven f-orbitals of the impurity ion were selected and moved, if required, to calculate the spin-orbital corrections using the CASSCF method. All seven f-orbitals were included in the active space for the correct calculation of their energies. The obtained orbitals were used at the third step for CASSCF

-NEVPT-calculation of $4f$-levels and transitions between them [8].

Since the value of the crystalline splitting of the f^{13} ion levels largely depends on the first sphere of ligands, the geometry of the central cluster (Tm or Yb)F_8 surrounded by a sphere of alkaline earth ions and point charges was optimized. The geometry was optimized using the Gaussian03 package with SDD (Tm, Yb, F) and LANL2MB (Ca, Sr, Ba) [9] basis sets.

Results

The optical properties of MeF_2-Tm^{2+} were studied in detail in a previous paper [10], in which a decrease in the energies of absorption lines of Tm^{2+} with increasing lattice constant was found.

Absorption of Yb^{3+}. Yb^{3+} replaces Me^{2+}, so it needs an additional negative charge to compensate. This charge is supplied, as a rule, by interstitial fluorine, which additionally splits the levels and change spectra of absorption and luminescence. In CaF_2-Yb^{3+} crystals, lines of cubic centers were identified in the paper [11] (Fig. 1). In SrF_2 and BaF_2 crystals, the lines of cubic centers clearly stand out against the background of lines of other centers (Fig. 1).

The dependences of the lines of cubic centers Yb^{3+} positions on the lattice constant converge linearly to the energy of atomic transitions (Fig. 2). Meanwhile, they intersect at the value of the interionic distance (Fig. 2), which is larger than for Tm^{2+} [10].

Luminescence Yb^{3+}. For Yb^{3+} in CaF_2 crystal, a large number of luminescence lines were observed in the luminescence spectrum (Fig. 3). The luminescence lines of cubic centers in CaF_2-Yb are marked with arrows [11]. The luminescence lines of cubic centers dominate in SrF_2 and BaF_2 crystals (Fig. 3). The luminescence Yb^{3+} lines converge with increasing lattice constant.

The $f-f$ lines of the Yb^{3+} ions are also excited in the vacuum ultraviolet area. By selecting the excitation wavelength in vacuum ultraviolet, it is possible to obtain practically single luminescence lines of Yb^{3+} cubic centers in all alkaline fluorides (Fig. 4). The wavelengths of the lines of cubic centers are the same as in the case of excitation of the $f-f$- area at 940ṅm (Fig. 3, 4).

The linear dependence of the positions of the luminescence lines on the lattice constant is very unusual, since the potential of a point charge varies as $1/r$.

Calculations

The calculated transition energies between the f- levels of free ions fairly agree with the experimental ones. The calculated energies of the $^2F_{7/2}-^2F_{5/2}$ transitions in free Tm^{2+} and Yb^{3+} ions are approximately 2–3% less than the experimental ones.

When Tm^{2+} and Yb^{3+} ions are placed in a crystalline environment, the initially degenerate levels $^2F_{7/2}$ and $^2F_{5/2}$ split in energy. However, the dependence of the level energy on the lattice constant calculated for an ideal lattice turns out to be nonlinear, as follows from the dependence of the charge potential on the distance to it. The calculated energy of transitions between levels also turns out to be nonlinear, which is inconsistent with the experimental linear dependences (Fig. 2). The calculated spin splitting - of the orbital levels by the crystal field decreases exponentially with increasing distance between the ions. When the lattice constant reaches approximately 7.5 Å for $Tm^{2+}E$ and 10 Å for Yb^{3+}, the splitting decreases almost to zero.

It was found that the distance to the ions of the nearest environment has a significant effect on the positions of the spins-orbital levels split by the crystal field. Since the central impurity ion remains the same in different lattices, the nearest environment should shift more toward the central ion (Tm^{2+} or Yb^{3+}) relative to the undistorted lattice with

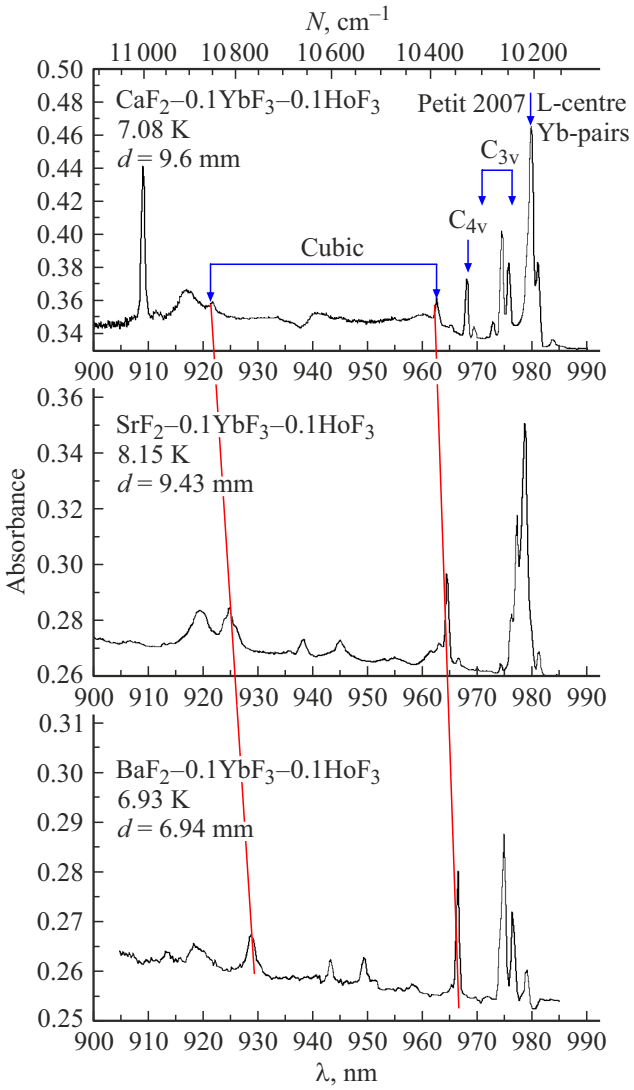

Figure 1. Absorption spectra of crystals $MeF_2-0.1$ mol.% $YbF_3-0.1\%$ HoF_3. Ho^{3+} ions have no absorption in this area, d — crystal thickness.

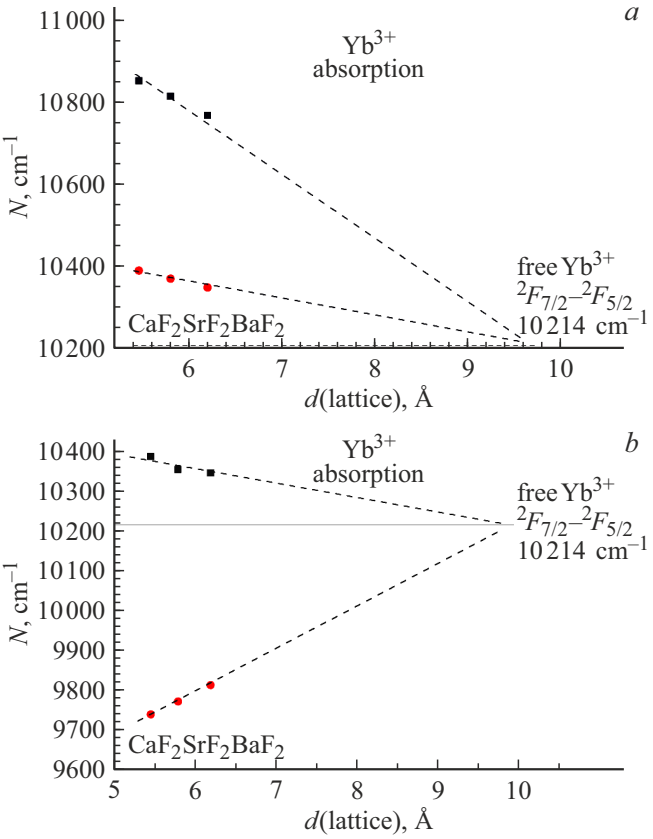

Figure 2. Dependence of the energy positions of the absorption (*a*) and luminescence (*b*) Yb^{3+} lines on the crystal lattice constant.

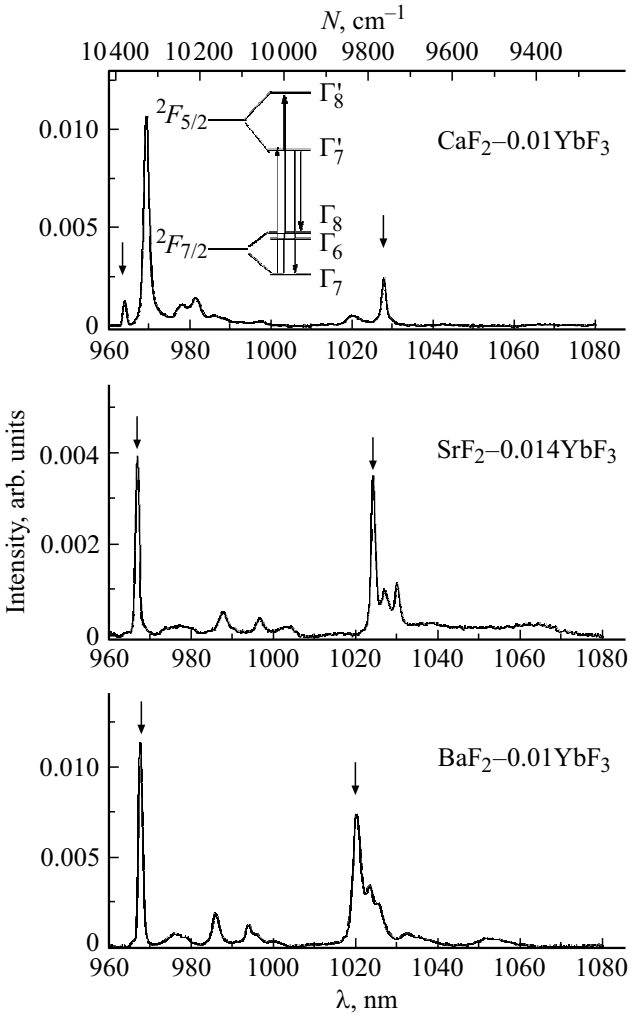

Figure 3. Luminescence spectra of crystals of alkaline earth fluorides MeF_2–0.01% YbF_3 at 85 K at 940 nm excitation. The insert shows the diagram of the energy levels of f^{13} (Tm^{2+} or Yb^{3+}) ions, and the arrows show the transitions during absorption and luminescence.

increasing lattice constant. For this reason, relaxation of the positions of the fluorine atoms closest to Tm^{2+} or Yb^{3+} in fluoride crystals CaF_2, SrF_2, BaF_2 was calculated (Fig. 5).

The positions of the nearest fluorine atoms were calculated using the Gaussian 03 program in the Yb^{2+}(or Tm^{2+}) F_8Me_{12} cluster. The positions of the central ion and the nearest fluorines varied, while the positions of the outer Me^{2+} were fixed.

For Yb^{3+} ions, the equilibrium distances to fluorine atoms are smaller than the lattice distances (Fig. 5) in all crystals. This fairly agrees with the smaller ionic radius I Yb^{3+} (0.98 Å) compared with the radii of the Ca^{2+} (1.26 Å), Sr^{2+} (1.4 Å), Ba^{2+} (1.56 Å) [12] alkaline earth ions. The calculated distances from the central impurity Tm^{2+} ion to the nearest fluorine are longer than the lattice distance in CaF_2 and shorter in BaF_2 (Fig. 5). This also agrees with the radius of the Tm^{2+} (1.3 Å [13]) ion. It is also important that the slope of the dependence of the calculated distances Tm–F or Yb–F on the distances in an ideal lattice is much less than one.

The use of the calculated distances to fluorine (Fig. 5) significantly improves the agreement between the theoretical and experimental results and leads to a linear dependence of the energies of the absorption and emission lines of the Tm^{2+} and Yb^{3+} ions on the lattice constant (Fig. 6).

Discussion

The order of the lower levels of Tm^{2+} is defined as $E_{3/2}$, $E_{1/2}$, G [14] (according to Bethe — D_7, D_6, D_8) or as D_7, D_8, D_6 [15,16]. The same sequence for the levels of Yb^{3+} in alkaline earth fluorides is followed in the papers [17,18]. It is assumed that transitions to D_6 in CaF_2–Tm^{2+} are forbidden and do not appear in the optical spectra [14–16]. At the same time, some weak long-wavelength bands in the luminescence spectra in MeF_2–Yb^{3+} are attributed to transitions to D_6 [17,18]. They can also belong to vibronic transitions [19]. According to our calculations, the levels D_8, D_6 are separated by 30–40 cm^{-1}, which is a small part of the energies of optical transitions 9000–10000 cm^{-1}.

With an increase in the interionic distance in alkaline earth metal fluoride crystals, the energy of the D_7–D'_7 and D_7–D'_8 transitions of the Tm^{2+} or Yb^{3+} ions decreases linearly, which is associated with a decrease in the crystal

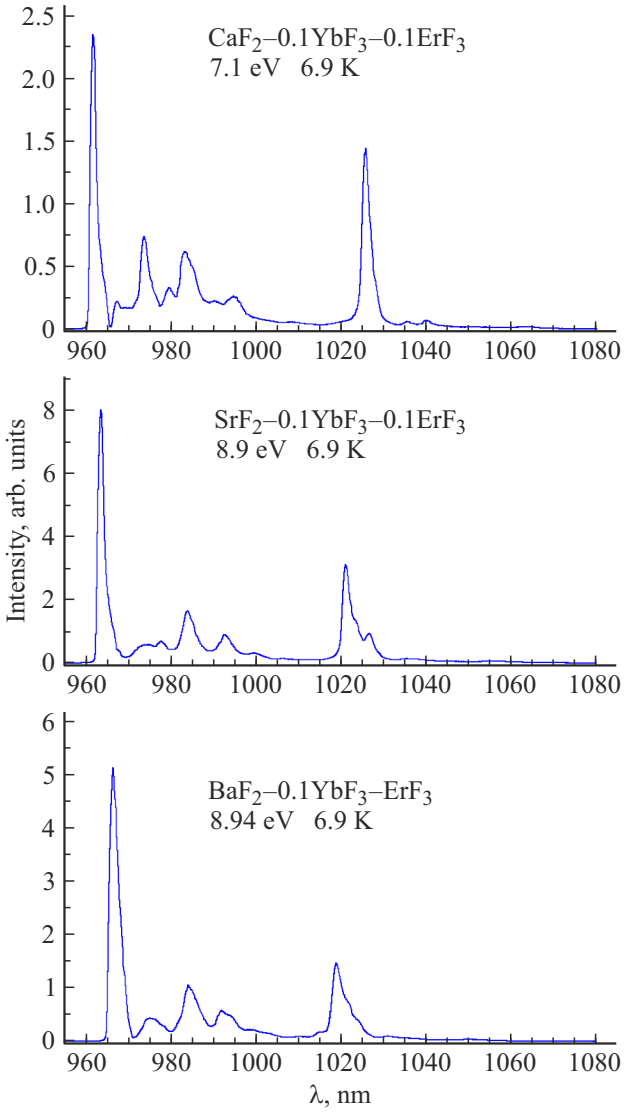

Figure 4. Luminescence spectra of $MeF_2-0.1$ mol.% Yb–Er crystals at 6.9 K upon vacuum ultraviolet excitation. Er^{3+} ions have no luminescence bands in this area.

splitting of the spin-orbital- of the $^2F_{7/2}$ and $^2F_{5/2}$ levels. The straight lines of both dependences converge at an energy of about 8780 cm^{-1} for Tm^{2+} [10] or 10200 cm^{-1} for Yb^{3+} (Fig. 2), which is close to the distance between the $^2F_{7/2}$ and $^2F_{5/2}$ levels in free ions (Fig. 2, *a*). There is another behavior for emission lines (Fig. 2, *b*). With an increase in the lattice constant, the energy of the long-wavelength line D'_7-D_8 increases, and the energy of the short-wave line D'_7-D_7 decreases. This behavior of the transition energies also agrees with a decrease in the crystalline splitting of states when emission transitions occur from the lower excited state to two split levels of the ground state. The observed changes in the positions of the luminescence lines are due to different slopes of the dependence of the levels $^2F_{5/2}$ (D_8, D_7) on the lattice constant. The lines of both dependences (Fig. 2, *b*, Fig. 6) also intersect at an energy close to the energy of the $^2F_{7/2}-^2F_{5/2}$transition in free ions (8774.02 cm^{-1} or 10214 cm^{-1} for Tm^{2+} and Yb^{3+} respectively [19,20]).

Taking into account the lattice distortion near the impurity ion, we obtained a fairly good agreement between the calculated experimental dependences (Fig. 6). The slopes of the linear dependence of line positions on the lattice constant are different for Yb^{3+} and Tm^{2+} ions (Fig. 6). A different slope of the dependences of the calculated distances from the Yb^{3+} and Tm^{2+} ions to neighboring fluorine atoms was also obtained by optimizing the geometry of the nearest environment (Fig. 5). The difference in the slopes of the dependences in Fig. 6 is due to the different radii of the impurity ions. The radius Tm^{2+} is equal to 1.3 Å, and the radius Yb^{3+} is — 0.98 Å; therefore, near Yb^{3+}, the lattice contracts more strongly and changes to a lesser extent with the change in the lattice constant (Fig. 5).

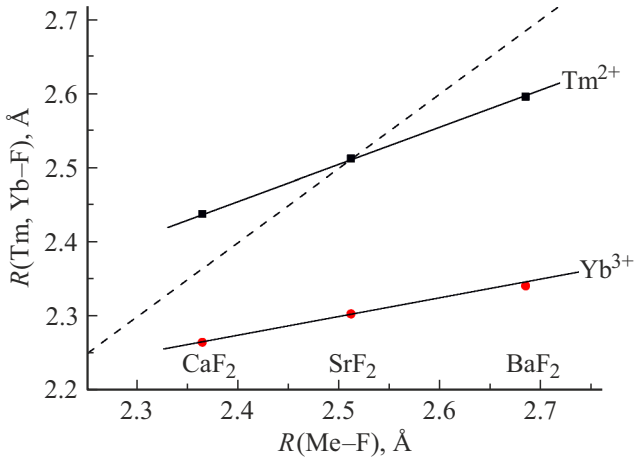

Figure 5. Calculated equilibrium distances from the central ion (Tm^{2+} or Yb^{3+}) to the nearest fluorine atoms depending on the distances in the undistorted lattice. The dependence for an ideal lattice is indicated by a dashed line.

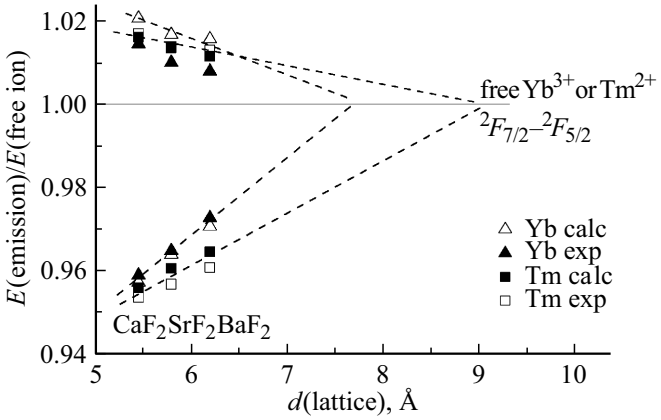

Figure 6. Dependence of the experimental and calculated luminescence lines of Tm^{2+} and Yb^{3+} on the lattice constant. The line energies are normalized to the energies of the $^2F_{7/2}-^2F_{5/2}$ transitions in free ions.

Conclusion

The optical spectra of $4f-4f$ - transitions of Yb^{3+} ions in fluoride crystals CaF_2, SrF_2, BaF_2 were studied. In fluoride crystals for Yb^{3+} ions, just as earlier for Tm^{2+} [10] ions, a linear decrease in the splitting of the spin-orbital - of the $^2F_{7/2}$, $^2F_{5/2}$ levels with increasing lattice constant was found. In contrast to the Tm^{2+} ions, the dependence of the splitting on the lattice constant for IYb^{3+} has a smaller slope, which is obviously related to the smaller size of the ytterbium ions.

The positions of the Tm^{2+} or Yb^{3+} bands in fluoride crystals are well described by ab initio CASSCF+NEVPT calculations taking into account the relaxation of the nearest sphere of fluorine atoms around the impurity ion.

Acknowledgments

In the work, we used the equipment of the - isotope shared use center for geochemical studies of the IGC SB RAS. The authors thank V.A. Kozlovsky for growing the crystals.

The paper was carried out as part of the project 0284-2021-0004 „Materials and technologies for the creation of radiation detectors, phosphors and optical glasses of the Russian Academy of Sciences“. The Institute of Solid State Physics, University of Latvia as the Center of Excellence, has received funding from the European Union's Horizon 2020 Framework Programme H2020-WIDESPREAD-01-2016-2017-TeamingPhase2 under grant agreement no. 739508, project CAMART2. The authors are grateful to K. Chernenko for help in carrying out the experiments at MAX IV.

Funding

The study was carried out as part of the implementation of the state assignment under the RAS Project 0284-2021-0004 The study of optical spectra in vacuum ultraviolet was carried out at the MAX IV Laboratory on Beamline FinEstBeams in accordance with the contract (Offer) 20200308.

Conflict of interest

The authors declare that they have no conflict of interest.

References

[1] H. Bethe. Annalen der Physik, **395** (2), 133 (1929).
[2] M.A. Elyashevich. *Spectra of Rare Earths* (GITTL, M., 1953) (in Russian).
[3] E.P. Merkx, M.P. Plokker, E. van der Kolk. Solar Energy Materials and Solar Cells, **223**, 110944 (2021).
[4] K.W. ten Kate, O.M. Krämer, E. van der Kolk. Solar Energy Materials and Solar Cells, **140**, 115 (2015).
[5] E. Radzhabov, V. Kozlovsky. Radiation Measurements, **122**, 6366 (2019). DOI: 10.1016/j.radmeas.2019. 01.013
[6] V. Pankratov, A. Kotlov. Nuclear Instruments and Methods in Phys. Research B: Beam Interactions with Materials and Atoms, **474**, 3540 (2020).
[7] F. Neese, F. Wennmohs, U. Becker, C. Riplinger. J. Chem. Phys., **152** (22), 224108 (2020).
[8] D. Aravena, M. Atanasov, V. Chilkuri, Y. Guo, J. Jung, D. Maganas, B. Mondal, I. Schapiro, K. Sivalingam, S. Ye et al. CASSCF Calculations in ORCA (4.2): A Tutorial Introduction. [Electronic resource] https://orcaforum.kofo.mpg.de/app.php/dlext/?cat=4.)
[9] M.J. Frisch et. al. *Gaussian 03* (Gaussian, Inc., Wallingford CT, 2003).
[10] E. Radzhabov, R. Shendrik, V. Pankratov. J. Lumin., **252**, 119271 (2022).
[11] V. Petit, P. Camy, J-L. Doualan, X. Portier, R. Moncorgé. Phys. Rev. B, **78**, 085131 (2008).
[12] R.D. Shannon. Acta Crystallographica A, **32** (5), 751767 (1976).
[13] Y. Jia. J. Solid State Chemistry, **95** (1), 184187 (1991).
[14] Z.J. Kiss. Phys. Rev., **127** (3), 718 (1962).
[15] B. Bleaney. Proc. Royal Society of London. Series A. Mathematical and Physical Sciences, **277** (1370), 289 (1964).
[16] W. Hayes, P. Smith. J. Phys. C: Solid State Physics, **4** (7), 840 (1971).
[17] M.L. Falin, K.I. Gerasimov, V.A. Latypov, A.M. Leushin. J. Phys.: Condensed Matter, **15** (17), 2833 (2003).
[18] K.I. Gerasimov, M.L. Falin. FTT, **51** (4), 681 (2009) (in Russian).
[19] I. Ignat′ev, V. Ovsyankin, J. Lumin., **72**, 679 (1997).
[20] W.C. Martin, R. Zalubas, L. Hagan. *Atomic Energy Levels — The Rare-Earth Elements*, Natl. Stand. Ref. Data Ser., Natl. Bur. Stand. (US), **60** (1), 1978.

Translated by E.Potapova